Control of neuronal oscillations via optogenetic stimulation

Numerical Optimal Control Project Report (SS 2019)

Diego Vieira, Felix Schmitt
Supervision: Florian Messerer, Prof. Moritz Diehl

***Abstract*—Oscillations are a prominent feature of neuronal activity, and are believed to play an important role in cognition as well as in neuronal disorders. Using an empirical model for hippocampal theta oscillations subject to optogenetic manipulation, we formulate and solve an optimal control problem to induce oscillations with arbitrary amplitude, phase and frequency modulation. We compare direct multiple shooting and model predictive control (MPC) approaches, and verify by means of simulations that MPC shows robustness to noise in the state variables and is able to partially compensate disturbances in the estimated model parameters. Finally, we evaluate different choices for the control cost factor in the objective function and for the evaluation interval and optimization horizon parameters.**

CONTENTS

I Introduction 1
I-A Motivation 1
I-B Model definition 2
I-C Optimization problem 3

II Methods 3
II-A Direct Multiple Shooting 3
II-B Model Predictive Control 3

III Results 3
III-A Sensitivity to state noise 3
III-B Sensitivity to parameter perturbations 3
III-C Effect of control cost factor 4

IV Discussion 4

References 5

I. INTRODUCTION

A. Motivation

Large-scale brain activity is characterized by neuronal oscillations, or brain rhythms, which arise from synchronized activity of neuronal populations. It is hypothesized that these rhythms help synchronize brain activity within and between brain regions, and play an important role in cognitive tasks and memory consolidation [1].

Among these rhythms, hippocampal theta waves are large oscillations (6–10 Hz in rodents) arising from excitatory-inhibitory neuronal interactions involving the medial septum, hippocampus and entorhinal cortex, which occur spontaneously during exploratory behavior and REM sleep [2]–[4]. In addition to participating in memory and spatial navigation [5], recent studies on animal models of temporal lobe epilepsy show that hippocampal theta periods occur more rarely and with an altered oscillatory frequency in these animals [6], [7].

In order to investigate the causal role of hippocampal theta in seizure occurrence and in the cognitive function of epileptic and healthy mice, we propose a method for the entrainment of neuronal oscillations by local optogenetic stimulation of excitatory cells in the hippocampus. Expanding on a previous study of optogenetic stimulation in the hippocampus [8], we have characterized the response for different stimulus intensities and frequencies in the 4–20 Hz frequency band in the recorded extracellular local field potential (LFP).

Our analysis reveals that sinusoidal stimulation elicits a narrow-banded oscillatory response at the frequency of stimulation. The power of the entrained oscillation is modulated by the stimulus amplitude in an almost-linear fashion for all tested frequencies, however with a large variability in the response due to changes in stimulus sensitivity and interaction with spontaneous oscillations [9].

By using a proportional-integral (PI) control loop, which modulates the stimulus intensity in real-time to minimize the difference between the measured response power and a reference target, we were able to reduce the response variability due to onset and brain state transitions [9]. This control scheme allows the experimenter to set a desired oscillatory power and automatically adjusts the stimulus to stabilize the response over long periods of time.

However, the control action and resulting input are still considerably noisy, due in large part to the measurement noise directly affecting the stimulation intensity. We would like to improve on this control algorithm, by including information from a model of the controlled system, and using this information to estimate the optimal control in real-time.

Within the scope of this project, our goals are to:

1) Formulate an optimal control problem
2) Implement the optimal control algorithm and validate it on the simulated system

3) Evaluate the controller sensitivity to state noise and model parameter deviations

B. Model definition

The system to be controlled exhibits an intrinsic oscillatory frequency ("spontaneous oscillation") and responds to external stimulation. A sketch of the modelled system is presented in Fig. 1.

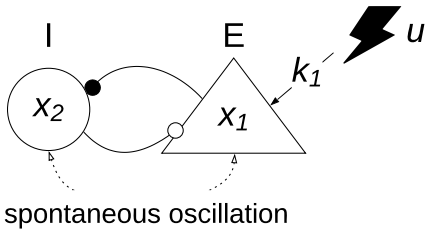

Fig. 1. Sketch of the modelled system.

The dynamics of these neuronal populations and their response to stimulation can be modelled as a perturbed oscillator, as described in Equation (1).

$$\begin{aligned} x &= (x_1, x_2)^\top, \quad \dot{x} = f(x, u) \\ \dot{x}_1 &= -x_2 \cdot \omega + x_1 \cdot (a - x_1^2 - x_2^2)/\tau + k_1 \cdot u + \eta_x \\ \dot{x}_2 &= \; x_1 \cdot \omega + x_2 \cdot (a - x_1^2 - x_2^2)/\tau + k_2 \cdot u + \eta_x \end{aligned} \tag{1}$$

where x_1 and x_2 (given in mV) are the real and imaginary states of an oscillator with an intrinsic natural frequency ω, radius $\sqrt{a}$, recovery time constant τ, k_1 and k_2 are the sensitivities to stimulation u, and η_x is i.i.d. noise in the state variables.

We can interpret x_1 and x_2 to be the activity of an excitatory and inhibitory neuronal population, respectively, as measured by an extracellular local field potential (LFP) recording electrode[1]. These two populations are recurrently connected with weights such that they exhibit a resonant frequency ω, and are excited by an external network (e.g., input from other hippocampal and afferent regions) to stabilize at an spontaneous oscillatory amplitude of $\sqrt{a}$. Our controller input u represents the effect of excitatory optogenetic stimulation[2], modulated by a gain k_1.

To simplify the analysis, we reduced the actuator dynamics to a simple additive term in the state derivative multiplied by a constant, and therefore refer to its magnitude in arbitrary units (a.u.), normalized to a range of $[0, 1]$. In a real setting, we would need to account for these dynamics, by either expanding the model, or by employing a feed-forward control block on the actuator.

The values used for the parameters are given in Table I.

Parameter	Value	Unit
ω	$6 \cdot 2\pi$	rad/s
a	0.01	mV^2
τ	0.1	s
k_1	100	$(\text{mV/s}) \cdot (\text{a.u.})^{-1}$
k_2	0	$(\text{mV/s}) \cdot (\text{a.u.})^{-1}$

TABLE I
MODEL PARAMETERS

These values were chosen to reflect the typical magnitude of the experimental data obtained by one of the authors. Note that k_2 is set to zero, since the optogenetic stimulation used in these experiments targeted exclusively the excitatory population. An example of the time and phase trajectories for the modeled system with different initial conditions is shown in Fig. 2.

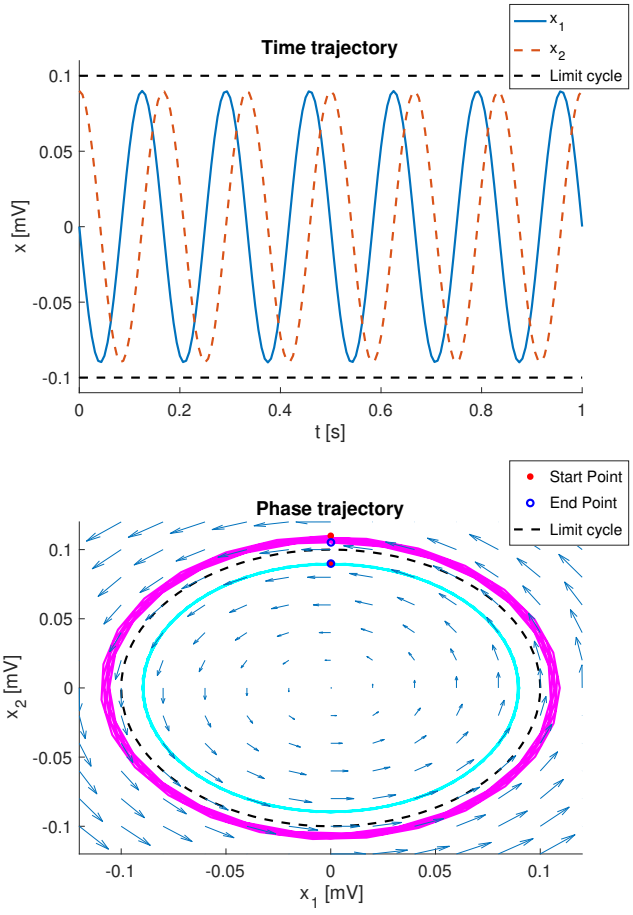

Fig. 2. Time and phase trajectories of the modelled system.

[1]As a rule, LFP recordings close to the neuronal body would show a negative deflection with higher neuronal activity. Here our state variables represent the LFP signals with inverted polarity (i.e., a more positive value reflects higher activity), to provide a more intuitive notation.

[2]Optogenetics is a technique in which a specific population of neurons are genetically manipulated to express light-sensitive ion channels, which make it possible to either excite or inhibit them by optical stimulation (see [10] for a review on the methods and [11] for the still incipient closed-loop applications).

C. Optimization problem

The goal of the controller is to minimize the error between the system output and a reference target oscillation, with a predetermined frequency, phase and amplitude, constrained to the modelled system dynamics and to the limitations of the applied stimulation intensity. The optimization problem is formulated in continuous time, with bounded control and no terminal cost:

$$\begin{aligned} \underset{x(\cdot),u(\cdot)}{\text{minimize}} \quad & \int_0^T L(x(t),u(t))dt \\ \text{subject to} \quad & x(0) - x_0 = 0 \\ & \dot{x}(t) - f(x(t),u(t)) = 0, \quad t \in [0,T] \\ & 0 \le u(t) \le 1 \end{aligned}$$

$$\begin{aligned} L(x(t),u(t)) &= (r(t) - x_1(t))^2 + \alpha \cdot u(t)^2 \\ r(t) &= a_{\text{ref}} \sin(\omega_{\text{ref}} t + \phi_{\text{ref}}) \\ a_{\text{ref}} &= 0.5 \text{ mV}, \quad \omega_{\text{ref}} = 8 \cdot 2\pi \text{ rad/s}, \quad \phi_{\text{ref}} = 0 \end{aligned}$$

II. Methods

We have formulated and investigated two solutions to the optimal control problem. First, by using a direct multiple shooting approach to find the optimal open-loop control for a given time horizon. Subsequently, by plugging in the multiple shooting solution into a feedback control loop using Model Predictive Control (MPC), so that the control trajectory can be dynamically adjusted in response to deviations in the state variables with respect to the model predictions.

We implemented the model and control algorithms using MATLAB and CasADi [12]. The source code for this project is available at https://github.com/divieira/noc_project.

A. Direct Multiple Shooting

In order to solve the proposed optimization problem, we used a direct multiple shooting approach. The model and cost function were discretized at a sampling frequency of $f_s = 160$ Hz using a single-step Runge-Kutta fourth-order method (RK4) integrator, with a constant control variable u_k per time step $t_s = 1/f_s$. The non linear program (NLP) was solved using an interior point method (IPOPT), yielding the piecewise constant optimal control trajectory $u(t) = u_k$, $t \in [kt_s, (k+1)t_s)$ for a given time horizon T.

B. Model Predictive Control

As an extension to the solution found by direct multiple shooting, we implemented the controller in a feedback loop using Model Predictive Control. At each interval of N_{shift} timesteps, the OCP is solved via multiple shooting for a horizon of N_{horizon} timesteps ahead, and the optimal control trajectory u found is applied until the next OCP evaluation. In order to increase computational efficiency, we warm start the controller by setting the initial conditions to the previously found solution shifted by N_{shift} steps, and limit the number of IPOPT iterations to 6 (median: 4 iterations). We set the horizon to 20 timesteps (1 period of the reference signal), and tested shift values of 1 and 5 timesteps.

III. Results

A. Sensitivity to state noise

The direct multiple shooting approach is able to find an optimal control trajectory, which closely follows the reference when the system is simulated without noise. However, since the control is calculated beforehand for the whole period (i.e., open-loop), it is not able to adapt to noise added to the state variables.

In order to evaluate the controller closer to a real world situation, Gaussian noise $\eta_x(k) = \mathcal{N}(0, t_s\sigma)$ was added at each time step to the output of the simulation (but not to the control model), resulting in a higher mean squared error (MSE) by 2 orders of magnitude (Fig. 3, left).

MPC, on the other hand, produces a marginally higher MSE in the noiseless scenario (since the objective function is evaluated for a shorter horizon). However, due to its feedback evaluation, it is able to react to unforeseen changes in the state variables and partially compensate for the error introduced by noise, achieving a reduction in the MSE by up to 1 order of magnitude when compared to the open-loop case, and a 5x reduction even with an evaluation interval corresponding to one quarter of a reference wave period (Fig. 3, center and right).

B. Sensitivity to parameter perturbations

Since the parameters of the physical system are unknown, in a real-world scenario they would need to be estimated, leading to deviations from values used in the OCP to the actual underlying values in the system dynamics (i.e., model-plant mismatch). We changed the parameters ω, a and k_1 to twice and half the nominal values used in the OCP solver. In order to make these effects more visible, we simulated the system without noise, for a direct multiple shooting approach and for MPC with evaluation intervals of 1 and 5 timesteps (Fig. 4).

Changes in the spontaneous oscillation amplitude a have no noticeable effect on the reference tracking, for both multiple shooting and MPC. However, changes in the spontaneous frequency ω or in the control input k_1 cause a tracking error in all control approaches tested. MPC with a single-timestep evaluation interval is partially able to compensate for most parameter perturbations, with a notably larger error induced by a reduction in the natural frequency ω. A longer evaluation interval leads to strong discontinuities and saturation in the control trajectory, and brings the error level close to that of open-loop control, with the simulations indicating that the controller is particularly sensitive to a decrease in ω or an increase in the sensitivity to control input k_1.

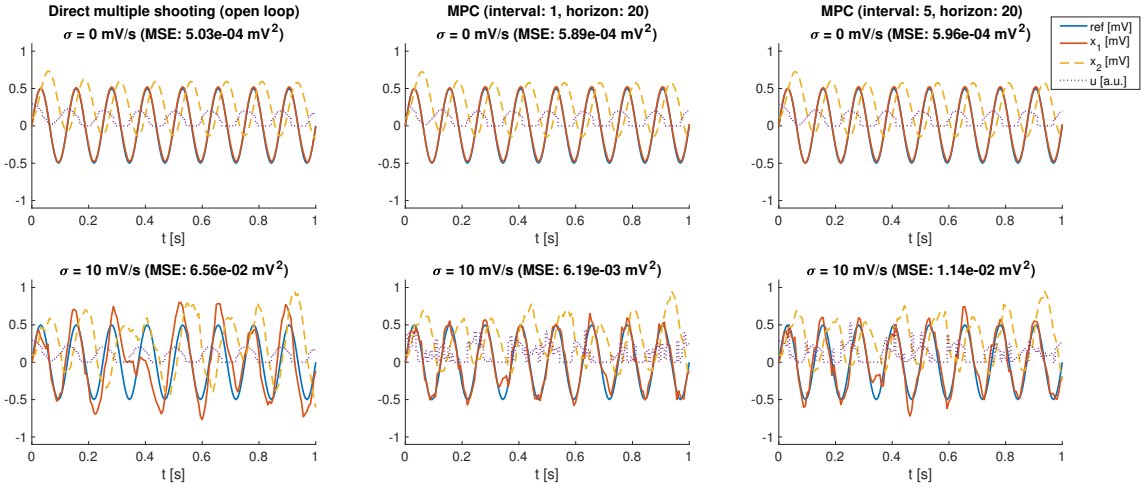

Fig. 3. Sensitivity to state noise. Comparison between direct multiple shooting (left) and MPC solutions with an evaluation interval of 1 (center) and 5 (right) timesteps in noiseless (top) and noisy (bottom) scenarios.

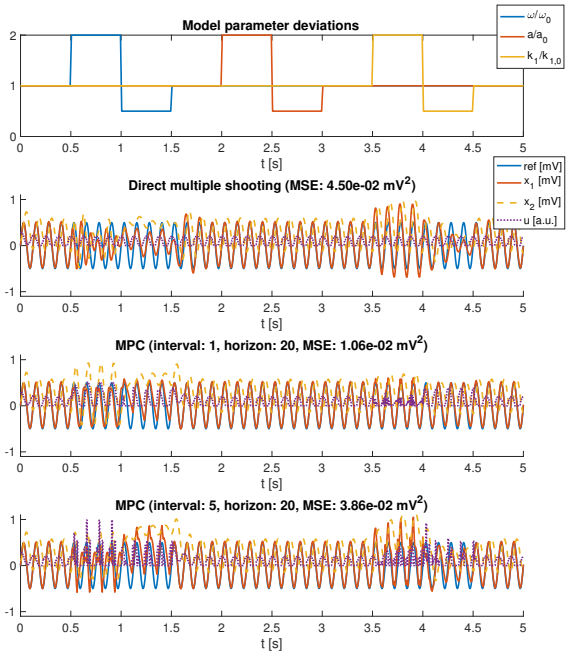

Fig. 4. Sensitivity to model parameter deviations. Comparison between direct multiple shooting and MPC with evaluation intervals of 1 and 5 timesteps to perturbations in the model parameters ω, a and k_1.

C. Effect of control cost factor

Finally, we also compared the mean-squared error (MSE) and mean control energy terms in the cost function $L(x, u)$ for different values of the cost balancing parameter α, and for different values of MPC control horizon and evaluation intervals (Fig. 5).

For approximately $\alpha \leq 0.1$ (the value used in the previous simulations), the MSE is close to minimum, with the exact amount depending on the evaluation interval and, to a smaller extent, on the optimization horizon. As we increase α, the MSE increases as the control energy approaches zero, reaching a maximum at approximately $\alpha \leq 100$. In this range, the evaluation interval has a larger influence than the horizon in both MSE and control energy, indicating that less frequent evaluations lead to a smaller control cost, which dominates the objective function for large α.

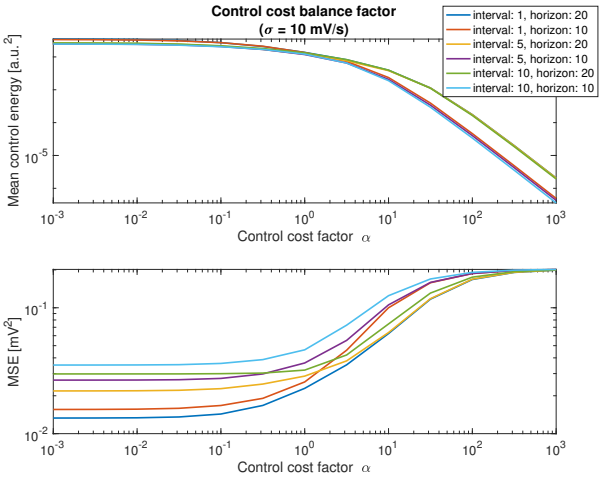

Fig. 5. Effect of control cost factor. MSE and mean control energy for different values of the control cost balancing factor α, for simulations with 1 s duration and noise level of σ = 10mV/s.

IV. Discussion

We have implemented a Model Predictive Control approach using direct multiple shooting and evaluated its performance on scenarios that present challenges in a real world usage. MPC is able to compensate for state noise and is robust to deviations in the model parameters when a unitary evaluation interval is used. For larger evaluation

intervals, which may be required due to computational or bandwidth constraints, the controller is especially sensitive to perturbations in the natural frequency ω and sensitivity to control input k_1. On the other hand, the small sensitivity to a for the recovery time constant τ used indicates that the corresponding term might be removed from the model equations, making the dynamics linear and allowing for more efficient methods, which can significantly accelerate the computation.

While we strived to keep the computational time of the simulations close to real-time, our implementation was slower than would be required for online control by about an order of magnitude on an average laptop computer. A speedup may be obtained by using real-time compilation, more efficient numerical solvers or a different control architecture (e.g., by using a linear model, as discussed above). However, other hardware and implementation requirements may further limit the capabilities of the MPC system, and will have to be taken into account for implementation.

While our analysis illustrates some of the issues the controller would have to respond to in actual usage, a more careful evaluation should be made by testing different combinations of noise and parameter deviations. Furthermore, this analysis could make use of additional information, such as the forward sensitivities from the numerical integrator, to provide more insight and allow for better quantification of the model-plant mismatch effects.

Finally, we assumed for the simulations presented here that the system structure is known. However, since we are employing an empirical model, the underlying dynamics might significantly differ from our model. Therefore, a complete validation of the solution must additionally require an evaluation of how well the online estimated model is able to capture the true system dynamics.

References

[1] G. Buzsáki and A. Draguhn, "Neuronal oscillations in cortical networks.," *Science (New York, N.Y.)*, vol. 304, no. 5679, pp. 1926–9, 2004. DOI: 10.1126/science.1099745.

[2] G. Buzsáki, *Theta oscillations in the hippocampus*, 2002. DOI: 10.1016/S0896-6273(02)00586-X.

[3] L. L. Colgin, "Mechanisms and Functions of Theta Rhythms," *Annual Review of Neuroscience*, vol. 36, no. 1, pp. 295–312, 2013. DOI: 10.1146/annurev-neuro-062012-170330.

[4] C. Müller and S. Remy, "Septo–hippocampal interaction," *Cell and Tissue Research*, vol. 373, no. 3, pp. 565–575, 2018. DOI: 10.1007/s00441-017-2745-2.

[5] G. Buzsáki and E. I. Moser, "Memory, navigation and theta rhythm in the hippocampal-entorhinal system," *Nature Neuroscience*, vol. 16, no. 2, pp. 130–138, 2013. DOI: 10.1038/nn.3304.

[6] L. V. Colom, A. García-Hernández, M. T. Castañeda, M. G. Perez-Cordova, and E. R. Garrido-Sanabria, "Septo-hippocampal networks in chronically epileptic rats: potential antiepileptic effects of theta rhythm generation.," *Journal of neurophysiology*, vol. 95, no. 6, pp. 3645–3653, 2006. DOI: 10.1152/jn.00040.2006.

[7] A. Kilias, U. Häussler, K. Heining, U. P. Froriep, C. A. Haas, and U. Egert, "Theta frequency decreases throughout the hippocampal formation in a focal epilepsy model," *Hippocampus*, 2018. DOI: 10.1002/hipo.22838.

[8] A. Kilias, A. Canales, U. P. Froriep, S. Park, U. Egert, and P. Anikeeva, "Optogenetic entrainment of neural oscillations with hybrid fiber probes," *Journal of Neural Engineering*, vol. 15, no. 5, 2018. DOI: 10.1088/1741-2552/aacdb9.

[9] D. Vieira, A. Killias, E. Paschen, P. Janz, U. Häussler, C. A. Haas, and U. Egert, "Entrainment of hippocampal theta oscillations by local optogenetic stimulation," in preparation.

[10] O. Yizhar, L. E. Fenno, T. J. Davidson, M. Mogri, and K. Deisseroth, "Optogenetics in Neural Systems," *Neuron*, vol. 71, no. 1, pp. 9–34, 2011. DOI: 10.1016/j.neuron.2011.06.004.

[11] L. Grosenick, J. H. Marshel, and K. Deisseroth, "Closed-Loop and Activity-Guided Optogenetic Control," *Neuron*, vol. 86, no. 1, pp. 106–139, 2015. DOI: 10.1016/j.neuron.2015.03.034.

[12] J. A. Andersson, J. Gillis, G. Horn, J. B. Rawlings, and M. Diehl, "Casadi: A software framework for nonlinear optimization and optimal control," *Mathematical Programming Computation*, vol. 11, no. 1, pp. 1–36, 2019.